

Impact of Methanol Adsorption on the Robustness of Analytical Supercritical Fluid Chromatography in Transfer from SFC to UHPSFC

Emelie Glenne, Marek Leško, Jörgen Samuelsson,* and Torgny Fornstedt*



Cite This: *Anal. Chem.* 2020, 92, 15429–15436



Read Online

ACCESS |



Metrics & More

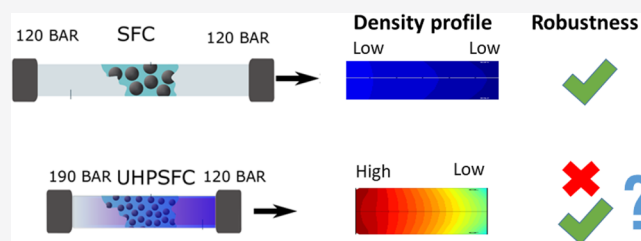


Article Recommendations



Supporting Information

ABSTRACT: In supercritical fluid chromatography (SFC), the retention of a solute depends on the temperature, density, pressure, and cosolvent fraction. Here, we investigate how the adsorption of the cosolvent MeOH changes with pressure and temperature and how this affects the retention of several solutes. The lower the pressure, the stronger the MeOH adsorption to the stationary phase; in addition, at low pressure, perturbing the pressure results in significant changes in the amounts of MeOH adsorbed to the stationary phase. The robustness of the solute retention was lowest when operating the systems at low pressures, high temperatures, and low cosolvent fractions in the eluent. Here, we found a clear relationship between the sensitivity of MeOH adsorption to the stationary phase and the robustness of the separation system. Finally, we show that going from classical SFC to ultrahigh-performance SFC (UHPSFC), that is, separations conducted with much smaller packing diameters, results in retention factors that are more sensitive to fluctuations in the flow rate than with traditional SFC. The calculated density profiles indicate only a slight density drop over the traditional SFC column (3%, visualized as lighter → darker blue in the TOC), whereas the drop for the UHPSFC one was considerably larger (20%, visualized as dark red → light green in the TOC). The corresponding temperature drops were calculated to be 0.8 and 6.5 °C for the SFC and UHPSFC systems, respectively. These increased density and temperature drops are the underlying reasons for the decreased robustness of UHPSFC.



INTRODUCTION

A trend seen in supercritical fluid chromatography (SFC), as in the transition from high-performance liquid chromatography (HPLC) to ultrahigh-performance liquid chromatography (UHPLC), is for the use of smaller particles to improve the efficiency and achieve better separation performance.¹ The use of sub-2 μm particles is often referred to as ultrahigh-performance SFC or UHPSFC. Compared with UHPLC, the pressure drop over the column is much smaller in UHPSFC. However, because of the compressibility of the fluid used in SFC, this additional pressure drop over the column could result in substantially larger density and viscosity gradients over the columns than those that are generally observed in UHPLC.^{1–3} Poe et al. reported that these gradients are more pronounced in columns packed with 3 μm -diameter particles than in those packed with 5 μm -diameter particles.⁴

In SFC, the fraction of the cosolvent in the eluent is often the most important factor controlling the retention.^{2,3,5} In a series of studies, we have investigated several different cosolvents in several different columns, exploring how they adsorb and how their adsorption affects the separation process in SFC.^{5–7} In these studies, we demonstrated that commonly used cosolvents adsorb to polar stationary phases, competing with the solute for available adsorption sites and hence affecting the solute retention and peak shape.^{6,7}

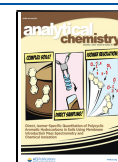
The temperature and pressure also influence the retention in SFC.^{3,8,9} The solute's solubility increases with increasing density;¹⁰ this will generally result in a reduction in the retention.¹¹ Increased pressure results in reduced retention because of the increasing density of the mobile phase. The effect of increasing temperature under constant pressure is more complicated: first, the retention increases because of decreasing mobile-phase density, and second, the retention decreases because of the exothermic nature of the adsorption process.^{9,12}

Here, we define robustness as the measure of a system's capacity to remain unaffected when control parameters are perturbed. In this study, we will use retention as a measure of the robustness of the system, while the control parameters that are perturbed are the temperature, pressure, and cosolvent fraction in the eluent. The possibility of adjusting an SFC separation using both temperature and pressure can be seen as a strength of SFC. However, this "flexibility" may also result in

Received: July 21, 2020

Accepted: October 29, 2020

Published: November 10, 2020



a less-robust separation system that may cause complications, for example, during scale-up¹³ or in technical transfer from SFC to UHPSFC.

The aim of this study is to investigate how the robustness of SFC separations is affected by pressure, temperature, and different co-solvent fractions. The focus will be to investigate how methanol (MeOH) adsorption is affected by pressure and temperature and how this adsorption affects the robustness of the separation. This will be done by determining MeOH adsorption to the column at several different pressures and temperatures and by investigating how the retentions of several solutes vary with temperature, pressure, and the amount of the cosolvent in the eluent. Finally, the same separation conducted using SFC and UHPSFC will be analyzed at different flow rates, with numerically calculated temperature and density profiles over the column.

THEORY

In this study, the two-component bi-Langmuir adsorption isotherm is used to describe cosolvent and solute adsorption. For the i -th compound in the mixture, the isotherm can be expressed as follows¹⁴

$$q_i = q_{s,I,i} \frac{K_{I,i} C_i}{1 + \sum_{j=1} K_{I,j} C_j} + q_{s,II,i} \frac{K_{II,i} C_i}{1 + \sum_{j=1} K_{II,j} C_j} \quad (1)$$

where K is the association equilibrium constant, q_s is the monolayer saturation capacity, C is the mobile-phase concentration, and q is the stationary-phase concentration.

In this case, the solute adsorption and cosolvent adsorption are described using a bi-Langmuir model, eq 1, while the solute retention factor at a specific concentration of the cosolvent in the eluent can be expressed as follows⁷

$$k_{\text{solute}} = Fq_{s,I} \frac{K_{I,\text{solute}}}{1 + K_{I,\text{co-solvent}} C_{\text{co-solvent}}} + Fq_{s,II} \frac{K_{II,\text{solute}}}{1 + K_{II,\text{co-solvent}} C_{\text{co-solvent}}} \quad (2)$$

where F is the phase ratio (i.e., ratio of the stationary and mobile phases in the column). The solute and cosolvent indices represent the solute and cosolvent bi-Langmuir adsorption parameters, respectively.

EXPERIMENTAL SECTION

Chemicals and Materials. Carbon dioxide (CO₂, 99.99%) was obtained from AGA Gas AB (Lidingö, Sweden), and HPLC-grade methanol (MeOH) (>99.9%) was obtained from Sigma-Aldrich (St. Louis, MO, USA). CO₂ was a liquid in the tube and was introduced into the SFC system via a dip tube in the cylinder. As solutes, caffeine (>99.0%), phenanthrene (>98%), catechol (>99%), bromacil (>98%), and carbazole (>95%) were used; all solutes were obtained from Sigma-Aldrich. The solvent 1,4-dioxane (>99.0%) was obtained from Merck (Darmstadt, Germany). The solutes are selected as they are common stable solutes used in SFC and with suitable retention times in the studies of separation systems.

A Kromasil diol column (150 × 4.6 mm) with 5 μm particles (SFC column) and a Kromasil diol column (100 × 3.0 mm) with 1.8 μm particles (UHPSFC column) (Nouryon, Bohus, Sweden) were used. Nitrous oxide (99.998%; Sigma-Aldrich) was used to determine the dead volume of the columns, according to Åsberg et al.³

The SFC system was an ACQUITY UPC2 (Waters Corporation, Milford, MA, USA) equipped with a PDA detector. A 10 μL loop was used for all injections. The mass flows of both the cosolvent and total eluent were measured using a CORI-FLOW M12 Coriolis mass flow meter (Bronkhorst High-Tech B.V., Ruurlo, Netherlands). The pressure was measured at the inlet and the outlet of the column using two EJX530A absolute pressure transmitters (Yokogawa Electric Corporation, Tokyo, Japan), with the *averaged pressure*, we mean the average of these measurements. The temperature was measured at 20, 50, and 80% of the column length, using three PT-100 four-wire resistance temperature detectors (Pentronic AB, Gunnebo, Sweden) with an accuracy of ±0.2 °C.

Procedures. The solute samples were first prepared as stock solutions of 1 g L⁻¹ solute in neat MeOH. The stock solutions were later diluted with 1,4-dioxane to a final concentration of 0.1 g L⁻¹ and filtered through a 0.45 μm polytetrafluoroethylene filter before injection. The solutes were detected at 220 nm, and 5 μL injections were made for the SFC experiments, and 2 μL injections were made for UHPSFC experiments. In all experiments, the column void volume was determined by injections of N₂O freshly bubbled through MeOH.

The effects of temperature, pressure, and amount of the cosolvent on the retention factor at a set flow rate of 1 mL min⁻¹ were investigated by injecting diluted samples of caffeine or carbazole under different conditions (see Figure 1). The

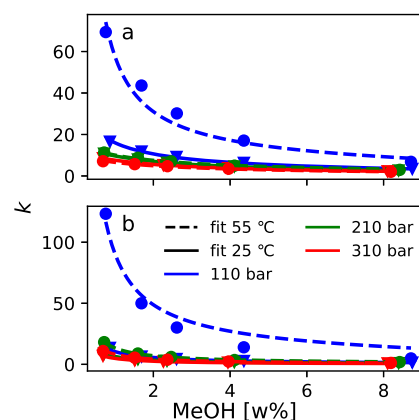


Figure 1. Retention factors of (a) carbazole and (b) caffeine eluted at set back pressures of 110 (blue lines), 210 (green lines), and 310 bar (red lines) and at set temperatures of 25 (solid lines) and 55 °C (dashed lines). The flow rate was set to 1 mL min⁻¹. Lines are fit to eq 2 (see the “Experimental Section” for more details).

investigated temperature was set to 25 or 55 °C, the back-pressure regulator pressure was set to 110, 210, or 310 bar, and the cosolvent fraction was set to 1, 2, 3, 5, 10, 15, or 20 v %.

In the design of experiments (DoE), presented in Figure 3, two designs were used per solute, both full-factorial designs in three levels with three center points. The concentration of the cosolvent eluent was 0.7–4.4 wt % (corresponding to the 1–5 v % set condition) in the first design and 8.1–17.8 wt % (corresponding to the 10–20 v % set condition) in the second design. The temperature was 25–55 °C, and the back-pressure regulator pressure was 110–310 bar. As the response, the logarithm of the retention factor of caffeine or carbazole was used. Regression models were constructed using MODDE 12

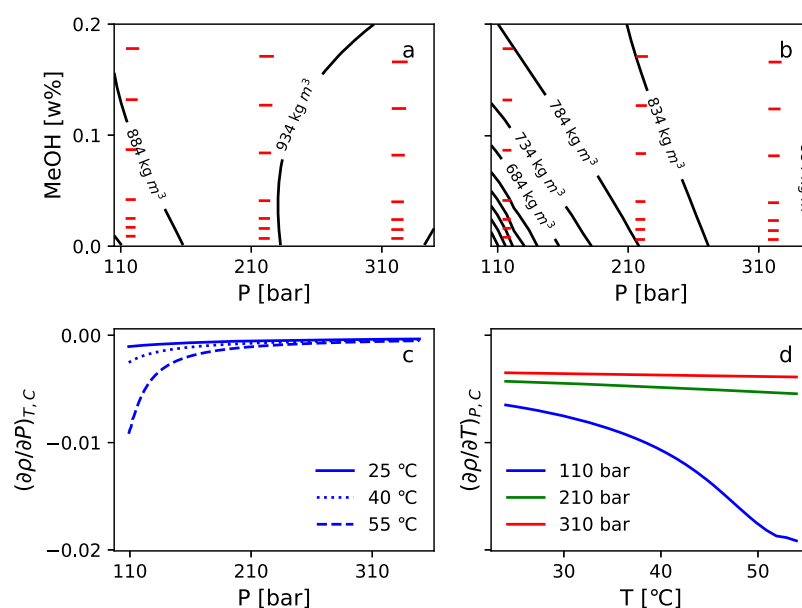


Figure 2. Isopycnic plot at (a) 25 and (b) 55 °C at pressures of 100–350 bar and with methanol fractions of 0–20 wt %. The red horizontal lines represent the measured mass fractions of methanol and measured pressures from the inlet to the outlet for the experiments run on the SFC column. (c) $(\partial\rho/\partial P)_{T,C}$ at temperatures of 25 (solid line), 40 (dotted line), and 55 °C (dashed line). (d) $(\partial\rho/\partial T)_{P,C}$ at pressures of 110 (blue line), 210 (green line), and 310 bar (red line).

software (Sartorius Stedim Biotech, Göttingen, Germany), after removing insignificant coefficients at a 95% confidence level to give

$$\log_{10} k = c_0 + c_T T + c_P P + c_C C + c_{T^2} T^2 + c_{P^2} P^2 + c_{C^2} C^2 + c_{PT} PT \quad (3)$$

where c_i is the coefficient, P is the pressure, T is the temperature, and C is the fraction of the modifier in the eluent (wt %). All regression models had excellent R^2 and Q^2 values (see Table S1 in the Supporting Information).

The adsorption isotherms shown in Figure 4 were estimated at 25 and 55 °C and at back pressures of 110, 210, and 310 bar. The adsorption data were determined using a combination of the recently improved elution by a characteristic point slope (ECP-slope)¹⁵ and the perturbation peak (PP) method;¹⁴ the former was used for low-concentration data and the latter was used for high-concentration data. In the PP method, 1.0 μL of neat MeOH was injected into a column already equilibrated with eluents containing MeOH fractions set to 1, 2, 3, 5, 10, 15, and 20 v %. In the ECP-slope approach, 6.0 μL of neat MeOH was injected into a column equilibrated with neat CO_2 . To convert the detector response into concentration, the UV response from injections of 2, 4, and 6 μL of MeOH was fitted to eq 4, so that the injected mass equaled the predicted eluted mass

$$C = k_1 \ln\left(\frac{k_2}{k_2 - R}\right) \quad (4)$$

where k_1 and k_2 are constants used in the calibration curve.¹⁶

Figure 5 shows the results for the 5 μm -particle SFC column and the 1.8 μm -particle UHPSFC column. The flow rate was set to 0.5, 1, 2, and 4 mL min^{-1} in the SFC experiments and to 0.25, 0.5, 0.75, 1, and 2 mL min^{-1} in the UHPSFC experiments; the temperature was set to 55 °C, and the pressure at the back-pressure regulator was set to 110 bar.

Calculations. The volumetric flow rate was calculated from the measured mass flow, and the density was calculated with the Knuz and Wagner equation¹⁷ of state implemented in REFPROP 10,¹⁸ using the average of the pressure and temperature measured in the column, together with the molar fractions of MeOH and CO_2 . The molar fractions were calculated from the mass flows, according to the previously reported method.^{5,7} The mass fraction of MeOH in the eluent was estimated from the ratio between the measured mass flow of MeOH and the total mass flow.

For robustness estimation (Figure 5), the standard deviations of retention factors (eq 3) were calculated at 10 different temperatures ranging from 25 to 55 °C and at 20 different pressures from 110 to 310 bar. At each investigated pressure and temperature, the retention factor was calculated for 1,000,000 virtual experiments. Each virtual experiment was generated using random perturbations of pressure, temperature, and the amount of the cosolvent in the eluent. The variations in the pressure, temperature, and fraction of the cosolvent in the eluent were assumed to be normally distributed and to have standard deviations of 2 bar, 0.5 °C, and 2.5% of the cosolvent fraction in the eluent, respectively. This was calculated for two different cosolvent fractions, 2.5 and 13 wt %, using the model derived for carbazole with small and large cosolvent fractions, respectively.

RESULTS AND DISCUSSION

This section is organized as follows. First, in the “Solute Retentions,” we will discuss the dependence of solute retentions on different temperatures, pressures, and cosolvent fractions in the eluent. Then, in the “Robustness Analysis,” we analyze the robustness of the separation system using DoE, and in the “Adsorption of MeOH,” we discuss methanol adsorption at different pressures and temperatures. Finally, in the “Transfer of SFC to UHPSFC,” separations conducted using a classical SFC column packed with 5 μm particles will be

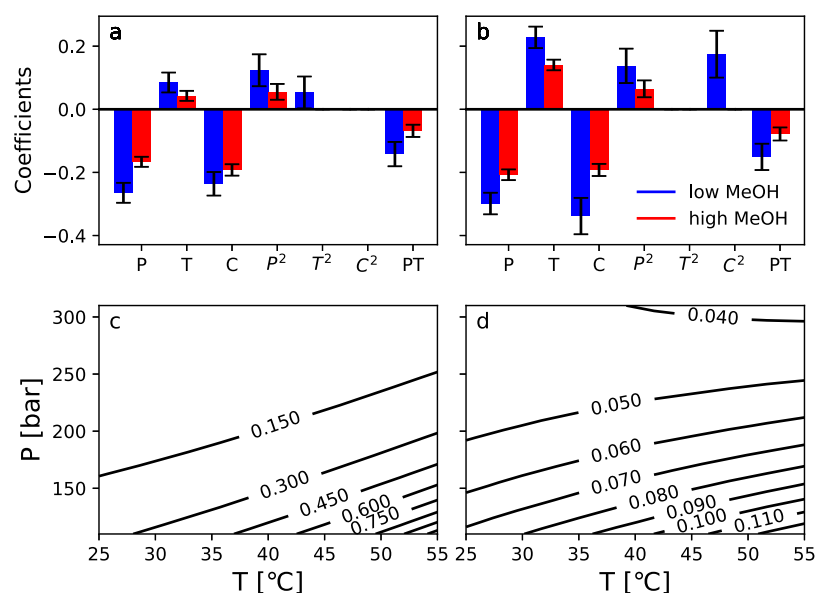


Figure 3. Scaled and centered coefficients of (a) carbazole and (b) caffeine for the retention model from the DoE with small methanol fractions (blue) and large methanol fractions (red) in the eluent. The standard deviation of the retention factor in controlled perturbations of temperature and pressure for the eluent with (c) 2.5 and (d) 13 wt % MeOH in the eluent. P is the pressure, T is the temperature, and C is the fraction of the modifier in the eluent (wt %). For more information, see Table S1 in the [Supporting Information](#).

compared with those using a UHPSFC column packed with 1.8 μm particles, at different flow rates.

Solute Retentions. The retention factors of carbazole (Figure 1a) and caffeine (Figure 1b) at back pressures of 110, 210, and 310 bar at temperatures of 25 and 55 $^{\circ}\text{C}$ for different MeOH fractions in the eluent are presented in Figure 1.

In Figure 1, one can see that with an increasing cosolvent fraction in the eluent, the retention factor decreases drastically, especially if the separation is conducted at a high temperature and low pressure. One can also observe that the separation system is more sensitive to changes in the pressure, temperature, and cosolvent fraction, if it is operated with a low cosolvent fraction in the eluent. The system becomes more stable as the fraction of the cosolvent in the eluent increases. However, the separation system's sensitivity to changes in the cosolvent fraction in the eluent decreases drastically with increasing pressure and decreasing temperature. In summary, the separation system is least robust to fluctuation in the cosolvent fraction, if it is operated at a low pressure and high temperature and using a small cosolvent fraction. See Figures S1–S5 in the Supporting Information for similar plots for phenanthrene, caffeine, bromacil, carbazole, and catechol. These plots also include retention data for 40 $^{\circ}\text{C}$ and set cosolvent fractions up to 20 v % MeOH. The results presented in the Supporting Information confirm the trends shown in Figure 1.

The retention factor is more sensitive to pressure changes, if the separation is conducted at low system pressures: compare the difference in retention as the pressure increases from 110 to 210 bar with the difference as the pressure increases from 210 to 310 bar. The same trend is noted for temperature, with a temperature reduction from 55 to 40 $^{\circ}\text{C}$ affecting the retention more than a reduction from 40 to 25 $^{\circ}\text{C}$ does (see Figures S1–S5 in the Supporting Information).

In SFC, the density is often seen as an important factor controlling the retention.^{19,20} We have previously shown that in many cases, the most important factor controlling the retention is the amount of the cosolvent in the eluent and

pressure and temperature generally have a less important role.^{3,8,21} The density as a function of the fraction of the cosolvent and temperature is presented for 25 $^{\circ}\text{C}$ in Figure 2a and 55 $^{\circ}\text{C}$ in Figure 2b.

The small horizontal lines in Figure 2a,b show the experiments conducted. In the most robust pressure region (310 bar in Figure 2a), perturbing the pressure, temperature, or cosolvent fraction results in only a slight change in density. In the least-robust region (110 bar in Figure 2b), even small changes in the pressure, temperature, or cosolvent fraction result in substantial density changes.

To better understand how the density is affected by pressure and temperature, we present the derivative of the density with pressure (Figure 2c) and temperature (Figure 2d) for 2.5 wt % cosolvent in the eluent. In Figure 2c, we clearly see that the density changes much more drastically with pressure, if the system is operated at a low pressure and high temperature. As the temperature increases, the change in density with pressure increases. In Figure 2d, one can observe that changing the temperature affects the density more drastically than changing the pressure does (compare Figure 2c,d). Here, the change in density with temperature at 110 bar is several times larger than the change in density with temperature at 210 and 310 bars.

Inspecting Figure 2c,d and considering that density is a major contributor to retention, we can now clearly understand that a robust separation should be conducted at a temperature and pressure at which small perturbations of temperature and pressure do not cause large density variations in the mobile phase. These regions are found at low temperatures up to around 40 $^{\circ}\text{C}$ and at high pressures exceeding 150 bar. The exact values at which these so-called robust regions are located depend on many factors, such as the separation system's response to changes in control parameters and the demand for maximum allowed variation in the separation.

Robustness Analysis. To investigate how temperature, pressure, and the fraction of the cosolvent in the eluent simultaneously affect the retention factors of both carbazole

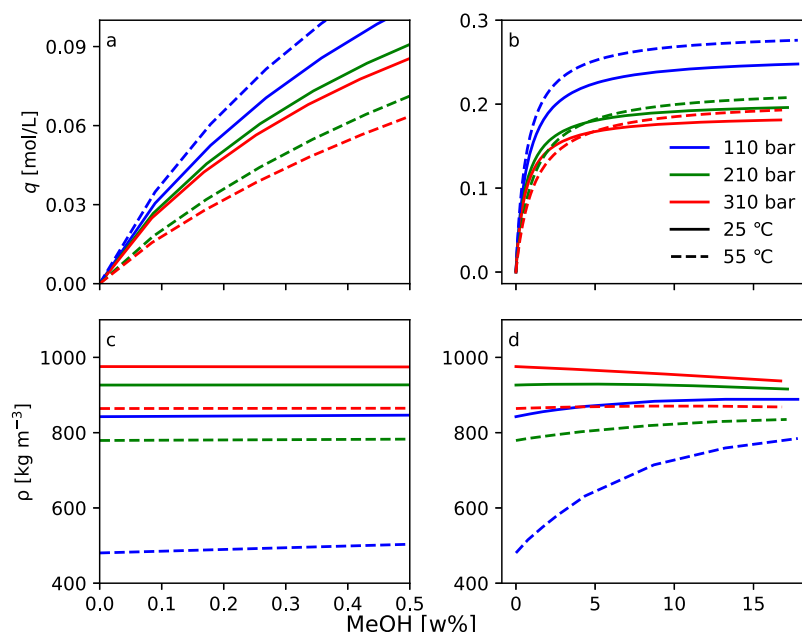


Figure 4. Adsorption isotherm for the SFC column measured at back pressures of 110 (blue), 210 (green), and 310 (red) bar and temperatures set to 25 (solid lines) and 55 °C (dashed lines). (a) Adsorption isotherm for methanol fractions of 0–0.5 wt % and (b) corresponding full measured range. (c,d) Calculated densities with methanol fractions corresponding to those in (a,b), respectively (see the “Experimental Section” for more details).

(Figure 3a) and caffeine (Figure 3b), the DoE was used to build a model.

Because of the nonlinear nature of the solute retention as a function of the amount of the cosolvent in the eluent, two designs were used. The first design considers low fractions of the cosolvent in the eluent (i.e., 0.7–4.4 wt %; Figure 3, blue bars) and the second design considers medium-to-high concentrations of co-solvent in the eluent (i.e., 8.1–17.8 wt %; Figure 3, red bars). In both designs, the pressure ranged from 110 to 310 bar and the temperature ranged from 25 to 55 °C. The retention was modeled using eq 3, and scaled and centered regression coefficients are presented graphically in Figure 3; their values are provided in Table S1 in the Supporting Information.

Comparing the model for the small fraction of the modifier (Figure 3, blue bars) with the model for the large fraction of the cosolvent (Figure 3, red bars), one can see that the coefficients are generally smaller in the system operating using larger fractions of the cosolvent in the eluent. This means that with larger fractions of the modifier, changes in pressure, temperature, and the amount of the cosolvent in the eluent will have smaller effects on retention. Inspecting, Figure 3a, the primary factors, we can see that pressure and the amount of the cosolvent in the eluent have approximately the same size of impact on retentions; similar trends are also observed in Figure 3b. For both solutes, temperature plays a less-important role in controlling the retention than the pressure or the amount of cosolvent does.

One difficulty is to define whether or not a system is robust. To study robustness, we used the retention model from the DoE to estimate how perturbations of the temperature, pressure, and cosolvent affect the retention, presenting the standard deviation of the estimated retention factors. This was done by randomly generating experiments with perturbations of the pressure, temperature, and amount of the cosolvent in the eluent (see the “Experimental Section” for more details).

The retention factor’s standard deviation is shown for carbazole at 2.5 wt % MeOH in the eluent in Figure 3c (using the model derived for low cosolvent fractions) and at 13 wt % MeOH in Figure 3d (using the model derived for high cosolvent fractions).

The observed standard deviations are much larger in the separation system operated at 2.5 wt % MeOH (Figure 3c) in the eluent than those in the one operated at 13 wt % MeOH (Figure 3d). The standard deviations at 110 bar and 55 °C are 1.27 and 0.13 at 2.5 and 13 wt % MeOH, respectively. The separation is nearly ten times more sensitive to perturbation, if it is conducted using the smaller fraction of MeOH in the mobile phase. From these robustness plots, we also clearly see that the standard deviation decreases drastically with increasing pressure and decreasing temperature. For example, at 200 bar and 40 °C, the standard deviations are 0.154 and 0.056 at 2.5 and 13 wt % MeOH, respectively, that is, a drop in standard deviation by more than eight times at 2.5 wt % MeOH and more than two times at 13 wt % MeOH.

Adsorption of MeOH. The drastic decrease in the retention factor with small modifier fractions, as seen in Figure 1, cannot be explained by drastic changes in the density because at 25 °C (Figure 2b), the density increases only modestly with the increasing cosolvent fraction in the eluent at 110 bar, is more or less constant at 210 bar, and decreases at 310 bar.

Figure 4 presents adsorption isotherms of MeOH at different pressures and temperatures. Figure 4a shows the adsorption isotherm up to 0.5 wt % cosolvent, and in Figure 4b, the whole measured concentration range is shown. Inspecting the initial part of the adsorption isotherm (Figure 4a), we observe that the adsorption is strongest at a low pressure (110 bar) and high temperature (55 °C; see the blue dashed line) and weakest at high pressure and temperature (310 bar and 55 °C; see the red dashed line). The initial adsorption decreases with increasing pressure at constant

temperature but increases with increasing temperature at constant pressure. Inspecting the whole adsorption isotherm (Figure 4b), we can clearly see a trend for decreasing saturation (extrapolating the maximum adsorbed amount from Figure 4b) with increasing temperature at constant pressure and with decreasing pressure at constant temperature.

The density of the mobile phase as a function of the eluent composition is presented in Figure 4c for the low-concentration range and in Figure 4d for the full concentration range. Assuming that the density controls the solubility of MeOH in the mobile phase, a low density would probably result in a larger degree of adsorption of MeOH on the stationary phase. The density is the lowest at 55 °C and 110 bar, which are also the conditions under which the equilibrium ratio is the highest (Figure 4a). However, the next lowest density is observed at 55 °C and 220 bar, the conditions under which the equilibrium ratio is among the lowest observed. Inspecting the full concentration range, up to around 17 wt % (see Figure 4d), the 55 °C and 110 bar conditions result in the highest adsorbed amount of MeOH on the stationary phase, that is, the lowest density conditions. We also see that the 25 °C and 310 bar conditions, which have the highest density, result in the lowest adsorption of MeOH on the stationary phase, in good agreement with the density solubility correlations. However, at 25 °C and 110 bar, the adsorption of MeOH on the stationary phase is much stronger than that observed at 55 °C and 210 and 310 bar, even though the density is lower. In other words, no clear correlation was observed between the adsorbed amount of MeOH and the density. However, if one instead considers the density at different pressures at a constant temperature, a clear pattern between the adsorbed amount and density can be observed. This clearly shows the dual nature of the temperature, as discussed in the Introduction.

From a robustness perspective, the system should be fairly robust in a region where the adsorption of MeOH does not drastically change. To further investigate the relationship between solute retention and cosolvent adsorption, the retention data presented in Figure 1 were fitted to eq 2 (see solid lines Figure 1). In general, we found a very good model fit to the retention, except at 110 bar and 55 °C, at which the fit was not perfect. This is probably due to two reasons: (i) the determined adsorption isotherm parameters, used in predicting the retention using eq 2, are dependent on the temperature, pressure, and density and therefore must be adjusted, if the system is not operated under isobaric, isopycnic, and isothermal conditions and (ii) in this region, the density is changing with changes in cosolvent fractions, so we expect some errors in the determined adsorption isotherm because it was not measured under isopycnic conditions. Furthermore, the uncertainties in the density estimated using the equation of state implemented in REFPROP are also larger. Tarafder et al. demonstrated that in this region, this error can approach 10%.²² Consequently, this error will also give rise to errors in the estimated adsorption isotherm, which will be manifested as errors in the retention predicted using eq 2.

With the knowledge that eq 2 can be used to estimate the retention, we can now analyze how the cosolvent adsorption affects the robustness. To investigate how sensitive a system is to changes in a parameter, the slope of the retention model relative to that parameter can be used. To investigate the sensitivity to the cosolvent fraction, the derivative of eq 2 is as follows

$$\left(\frac{\partial k_{\text{solute}}}{\partial C_{\text{co-solvent}}}\right) = -Fq_{s,I} \frac{K_{I,\text{co-solvent}} K_{I,\text{solute}}}{(1 + K_{I,\text{co-solvent}} C_{\text{co-solvent}})^2} - Fq_{s,II} \frac{K_{II,\text{co-solvent}} K_{II,\text{solute}}}{(1 + K_{II,\text{co-solvent}} C_{\text{co-solvent}})^2} \quad (5)$$

Equation 5 clearly shows that the system becomes more stable with the increasing cosolvent fraction (i.e., the denominator becomes larger). This clearly shows that the separation system's sensitivity to MeOH perturbations in the eluent decreases with an increasing amount of MeOH in the eluent, as was also observed in Figure 3. This result indicates that the stronger the MeOH adsorbs to the stationary phase, the less robust the system will be.

Transfer of SFC to UHPSFC. The current trend in SFC is to conduct separation using smaller packing particles. Here, this was investigated by comparing columns packed with 5 μm versus 1.8 μm particles but having the same phase chemistry. To reduce the pressure drop over the UHPSFC system, the 1.8 μm particles were packed in a 100 \times 3 mm column, while in the SFC system, the 5 μm particles were packed in a 150 \times 4.6 mm classical column.

Figure 5 shows the normalized retention factors at different linear flow rates for both the 5 μm packing (solid lines) and 1.8

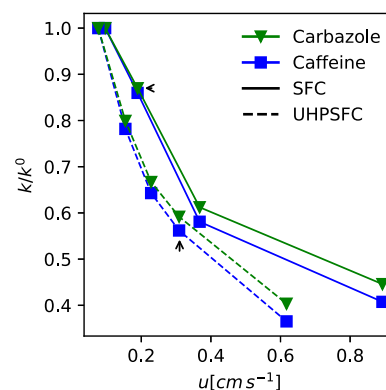


Figure 5. Normalized retention factors of carbazole (green) and caffeine (blue) in UHPSFC (dashed lines) and SFC (solid lines) columns vs the linear flow rate. The flow rate was set to 0.5, 1, 2, and 4 mL min^{-1} in the SFC system and 0.25, 0.5, 0.75, 1, and 2 mL min^{-1} in the UHPSFC system. The back pressure was set to 110 bar, and the temperature was set to 55 °C. The arrows indicate measurements made at a flow rate of 1 mL min^{-1} (see the “Experimental Section” for more details).

μm packing (dashed lines) at 55 °C and a back pressure of 110 bar. The flow rate was set to 0.5, 1, 2, and 4 mL min^{-1} for the SFC column and 0.25, 0.5, 0.75, 1, and 2 mL min^{-1} for the UHPSFC column. Interestingly, in Figure 5, we can see that the retention factor is more sensitive to flow rate changes in the UHPSFC than in the SFC column.

The main difference between SFC and UHPSFC is the pressure. The average pressure, that is, the averaged measured inlet and outlet pressures, over the column increases from 114 bar at the lowest flow rate to 164 bar at the highest flow rate in the SFC system. In the UHPSFC system, the average pressure increases from 119 to 191 bar with the increasing flow rate. At the lowest flow rate, the pressure drop was 13 bar over the UHPSFC column and 1.9 bar over the SFC column, and at a flow rate of 2 mL min^{-1} , the pressure drop was 136 bar in the UHPSFC column and only 10 bar in the SFC column. In the

SFC column, the highest pressure drop was observed at 31 bar, a flow rate of 4 mL min⁻¹, and a temperature of 25 °C. To investigate how this pressure drop affects the density and temperature profiles over the columns, these profiles were calculated (see the “Calculations for TOC” in page S6, in the Supporting Information).

In the analytical SFC system (top system in the TOC), we had a very small degree of radial and axial density and temperature gradients as compared to those in the UHPSFC system (bottom system in the TOC). In the latter system, we could only conduct the separation up to a set flow rate of 2 mL min⁻¹ because of the system's maximum pressure limit, compared with the SFC case, in which we conducted the separation up to a set flow rate of 4 mL min⁻¹, which is the maximum allowed flow rate of the system. In other words, to utilize smaller packing, we are forced to use a lower back pressure to increase the throughput at the cost of operating the system in a more unstable region. Some practical guidelines according to this discussion are given in the Conclusions.

CONCLUSIONS

The robustness of SFC separation conducted at different temperatures, pressures, and cosolvent concentrations in the eluent was discussed.

Solute retention as a function of pressure, temperature, and the amount of the cosolvent in the eluent was modeled using the DoE. With this model, the robustness of the system, which varies with pressure, temperature, and the amount of the cosolvent in the eluent, was studied. In this case, the robustness was nearly ten times higher when conducting the separation at 13 wt % MeOH in the eluent than that at 2.5 wt %. The robustness also increased more than eight times when increasing the pressure from 110 to 200 bar and decreasing the temperature from 55 to 40 °C.

One of the most important factors controlling the retention is the adsorption of MeOH to the stationary phase. Here, we demonstrated that the MeOH adsorption is strongly dependent on the pressure and temperature without any clear correlation with the mobile-phase density. However, the adsorption of MeOH to the stationary phase generally decreases with increasing pressure at a constant temperature and increases with increasing temperature at a constant pressure.

Compared with separations conducted using SFC, separations using UHPSFC are generally less-robust because of the larger pressure drop over the column. Calculated density profiles showed a density drop over the column at 110 bar and 55 °C of 20% in the UHPSFC column and 3% in the SFC column. The calculated temperature drop over the column under the same conditions was 6.5 °C in the UHPSFC system and only 0.8 °C in the SFC system. To reduce these gradients and increase the robustness, the separation could be conducted at a higher set back pressure. However, because of a higher pressure drop over the UHPSFC column and limitations in the system pressure, this might force the separation to be conducted at a lower flow rate.

The technical transfer of separations could result in retention factor shifts and force us to operate the system under less-robust conditions. To mitigate this risk, we could do the following: (1) select operational conditions for the separation systems at low temperatures using as high a back pressure as possible and (2) select stationary phases with

column chemistries, allowing avoidance of conducting the separation at very low cosolvent fractions.

ASSOCIATED CONTENT

Supporting Information

The Supporting Information is available free of charge at <https://pubs.acs.org/doi/10.1021/acs.analchem.0c03106>.

Retention factors of small-size injections of the selected model compounds eluted at different set back pressures (110, 210, and 310 bar) and different set temperatures 25, 40, and 55 °C: phenanthrene, caffeine, bromacil, carbazole, and catechol; Calculations for TOC: *temperature and density distributions in the column*; and table with scaled and centered regression coefficients for all responses and the quality of the fit in terms of variation explained by the models used in the manuscript (PDF)

AUTHOR INFORMATION

Corresponding Authors

Jörgen Samuelsson – Department of Engineering and Chemical Sciences, Karlstad University, SE-651 88 Karlstad, Sweden; Phone: +46 54700 1620; Email: Jorgen.Samuelsson@kau.se

Torgny Fornstedt – Department of Engineering and Chemical Sciences, Karlstad University, SE-651 88 Karlstad, Sweden; orcid.org/0000-0002-7123-2066; Phone: +46 54 700 1960; Email: Torgny.Fornstedt@kau.se

Authors

Emelie Glenne – Department of Engineering and Chemical Sciences, Karlstad University, SE-651 88 Karlstad, Sweden

Marek Leško – Department of Engineering and Chemical Sciences, Karlstad University, SE-651 88 Karlstad, Sweden

Complete contact information is available at:

<https://pubs.acs.org/doi/10.1021/acs.analchem.0c03106>

Author Contributions

The manuscript was written jointly by all the authors, who have approved the current version of the manuscript.

Notes

The authors declare no competing financial interest.

ACKNOWLEDGMENTS

This work was supported by the Swedish Knowledge Foundation via the KKS SYNERGY project “BIO-QC: Quality Control and Purification for New Biological Drugs” (grant number 20170059) and by the Swedish Research Council (VR) via the project “Fundamental Studies on Molecular Interactions aimed at Preparative Separations and Biospecific Measurements” (grant number 2015-04627).

REFERENCES

- (1) Åsberg, D.; Samuelsson, J.; Leško, M.; Cavazzini, A.; Kaczmarek, K.; Fornstedt, T. *J. Chromatogr. A* **2015**, *1401*, 52–59.
- (2) Enmark, M.; Glenne, E.; Leško, M.; Langborg Weinmann, A.; Leek, T.; Kaczmarek, K.; Klarqvist, M.; Samuelsson, J.; Fornstedt, T. *J. Chromatogr. A* **2018**, *1568*, 177–187.
- (3) Åsberg, D.; Enmark, M.; Samuelsson, J.; Fornstedt, T. *J. Chromatogr. A* **2014**, *1374*, 254–260.
- (4) Poe, D. P.; Veit, D.; Ranger, M.; Kaczmarek, K.; Tarafder, A.; Guiochon, G. *J. Chromatogr. A* **2014**, *1323*, 143–156.
- (5) Glenne, E.; Öhlén, K.; Leek, H.; Klarqvist, M.; Samuelsson, J.; Fornstedt, T. *J. Chromatogr. A* **2016**, *1442*, 129–139.

- (6) Glenne, E.; Leek, H.; Klarqvist, M.; Samuelsson, J.; Fornstedt, T. *J. Chromatogr. A* **2017**, *1496*, 141–149.
- (7) Glenne, E.; Leek, H.; Klarqvist, M.; Samuelsson, J.; Fornstedt, T. *J. Chromatogr. A* **2016**, *1468*, 200–208.
- (8) Forss, E.; Haupt, D.; StÅlberg, O.; Enmark, M.; Samuelsson, J.; Fornstedt, T. *J. Chromatogr. A* **2017**, *1499*, 165–173.
- (9) Muscat Galea, C.; Slosse, A.; Mangelings, D.; Vander Heyden, Y. *J. Chromatogr. A* **2017**, *1518*, 78–88.
- (10) Taberner, A.; Vieira de Melo, S. A. B.; Mammucari, R.; Martín del Valle, E. M.; Foster, N. R. *J. Supercrit. Fluids* **2014**, *93*, 91–102.
- (11) Tarafder, A.; Guiochon, G. *J. Chromatogr. A* **2011**, *1218*, 4569–4575.
- (12) Zou, W.; Dorsey, J. G.; Chester, T. L. *Anal. Chem.* **2000**, *72*, 3620–3626.
- (13) Enmark, M.; Åsberg, D.; Leek, H.; Öhlén, K.; Klarqvist, M.; Samuelsson, J.; Fornstedt, T. *J. Chromatogr. A* **2015**, *1425*, 280–286.
- (14) Guiochon, G.; Shirazi, D. G.; Felinger, A.; Katti, A. M. *Fundamentals of Preparative and Nonlinear Chromatography*, 2nd ed.; Academic Press: Boston, MA, 2006.
- (15) Samuelsson, J.; Undin, T.; Törnåcrona, A.; Fornstedt, T. *J. Chromatogr. A* **2010**, *1217*, 7215–7221.
- (16) Ottiger, S.; Kluge, J.; Rajendran, A.; Mazzotti, M. *J. Chromatogr. A* **2007**, *1162*, 74–82.
- (17) Kunz, O.; Klimeck, R.; Wagner, W.; Jaeschke, M. The GERG-2004 Wide-Range Equation of State for Natural Gases and Other Mixtures. *GERG Technical Monograph 15*; Fortschritt-Berichte VDI, VDI-Verlag: Düsseldorf, 2007.
- (18) Lemmon, E. W.; Bell, I. H.; Huber, M. L.; McLinden, M. O. *NIST Standard Reference Database 23: Reference Fluid Thermodynamic and Transport Properties-REFPROP, Version 10.0*; National Institute of Standards and Technology, Standard Reference Data Program: Gaithersburg, 2018.
- (19) Tarafder, A.; Hill, J. F.; Iraneta, P. C.; Fountain, K. J. *J. Chromatogr. A* **2015**, *1406*, 316–323.
- (20) Bartle, K. D.; Clifford, A. A.; Jafar, S. A. *J. Chem. Eng. Data* **1990**, *35*, 355–360.
- (21) Enmark, M.; Åsberg, D.; Samuelsson, J.; Fornstedt, T. *Chromatogr. Today* **2014**, *8*, 14–17.
- (22) Tarafder, A.; Kaczmarzski, K.; Poe, D. P.; Guiochon, G. *J. Chromatogr. A* **2012**, *1258*, 136–151.